Bioconjugate Chemistry

Article

pubs.acs.org/bc

Conjugates of Amino Acids and Peptides with 5-*O*-Mycaminosyltylonolide and Their Interaction with the Ribosomal Exit Tunnel

Anna Shishkina,[†] Gennady Makarov,[‡] Andrey Tereshchenkov,[‡] Galina Korshunova,[†] Nataliya Sumbatyan,[‡] Andrey Golovin,[§] Maxim Svetlov,[∥] and Alexey Bogdanov*[,†,§]

[†]A.N. Belozersky Institute of Physico-Chemical Biology, Lomonosov Moscow State University, Leninskie Gory, 1, bldg 40, 119992 Moscow, Russia

[‡]Department of Chemistry, Lomonosov Moscow State University, Leninskie Gory, 1, bldg 3, 119991 Moscow, Russia

[§]Department of Bioengineering and Bioinformatics, Lomonosov Moscow State University, Leninskie Gory, 1, bldg 43, 119992 Moscow, Russia

[∥]The Institute of Protein Research, Russian Academy of Sciences, Institutskaya st., 4, 142290 Pushchino, Moscow Region, Russia

Supporting Information

ABSTRACT: During protein synthesis the nascent polypeptide chain (NC) extends through the ribosomal exit tunnel (NPET). Also, the large group of macrolide antibiotics binds in the nascent peptide exit tunnel. In some cases interaction of NC with NPET leads to the ribosome stalling, a significant event in regulation of translation. In other cases NC−ribosome interactions lead to pauses in translation that play an important role in cotranslational folding of polypeptides emerging from the ribosome. The precise mechanism of NC recognition in NPET as well as factors that determine NC conformation in the ribosomal tunnel are unknown. A number of derivatives of the macrolide antibiotic 5-*O*-mycaminosyltylonolide (OMT) containing *N*-acylated amino acid or peptide residues were synthesized in order to study potential sites of NC−NPET interactions. The target compounds were prepared by conjugation of protected amino acids and peptides with the C23 hydroxyl group of the macrolide. These OMT derivatives showed high although varying abilities to inhibit the firefly luciferase synthesis *in vitro*. Three glycil-containing derivatives appeared to be strong inhibitors of translation, more potent than parental OMT. Molecular dynamics (MD) simulation of complexes of tylosin, OMT, and some of OMT derivatives with the large ribosomal subunit of *E. coli* illuminated a plausible reason for the high inhibitory activity of Boc-Gly-OMT. In addition, the MD study detected a new putative site of interaction of the nascent polypeptide chain with the NPET walls.

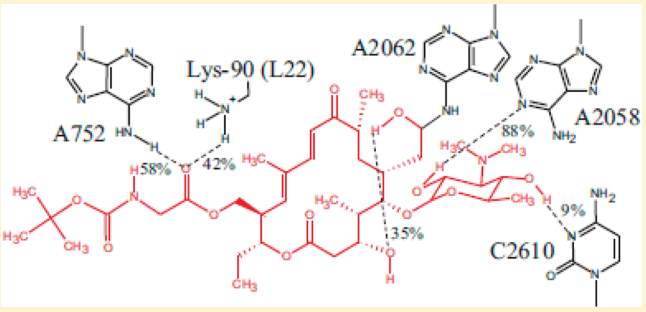

INTRODUCTION

The polypeptide chain of a protein which is synthesized at the peptidyl transferase center (PTC) of the ribosome moves along the ribosomal exit tunnel (NPET) as the nascent peptide is elongated. NPET spans the body of the large ribosomal subunit from PTC to the exit point where NC becomes available for interaction with chaperones and targeting factors. The primary functional role of the ribosomal tunnel is to ensure advancement of any newly synthesized polypeptide chain from PTC to the NPET exit. Nevertheless, side chains of nascent peptides appear to interact with tunnel walls; in some cases NC exhibits interactions with NPET components which are so strong and specific that they lead to a translation arrest followed by alterations in the expression level of some genes.[1−3] To date two NPET regions were revealed to be crucial for ribosome stalling. The first region is composed of 23S rRNA nucleotide residues which form part of the so-called outer layer of PTC, whereas the second one is located at the constricted segment of NPET consisting not only of the 23S rRNA nucleotide residues, but also of the amino acid residues of the ribosomal proteins L4 and L22.[2] These regulatory regions of NPET overlap with the binding sites of macrolide antibiotics, hampering the progression of nascent chains by blocking the tunnel.

Macrolides are members of a large family of natural and semisynthetic antibiotics that target the ribosome. They contain a 12-, 14-, 15-, or 16- membered macrolactone ring and one or more sugar moieties.[4] Once atomic structure of bacterial ribosomes was resolved, macrolide complexes with the 50S subunits of bacterial ribosomes were subjected to rigorous

Received: May 14, 2013
Revised: September 23, 2013
Published: October 4, 2013

   dx.doi.org/10.1021/bc400236n | *Bioconjugate Chem.* 2013, 24, 1861−1869

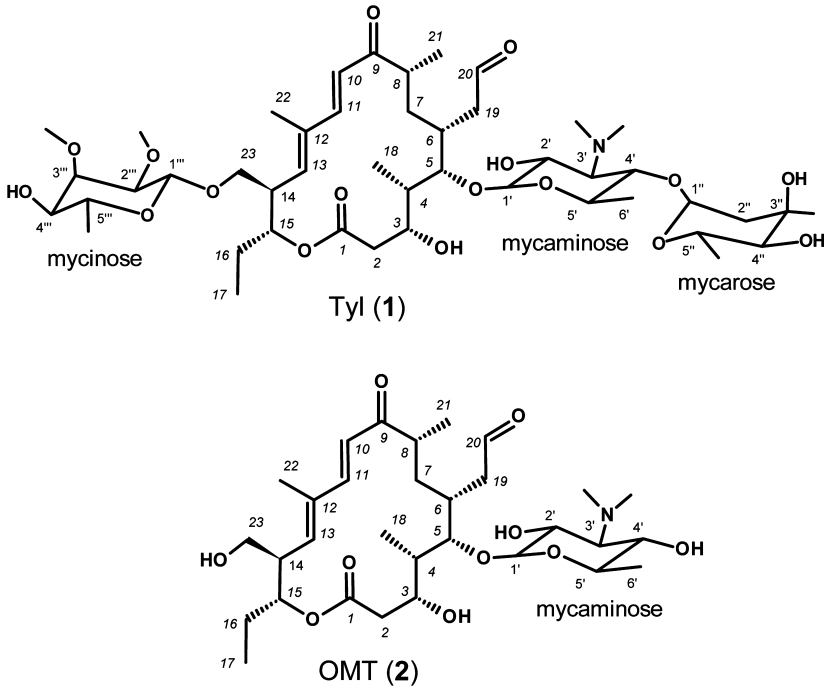

Figure 1. Chemical structures of tylosin (**1**) and OMT (**2**).

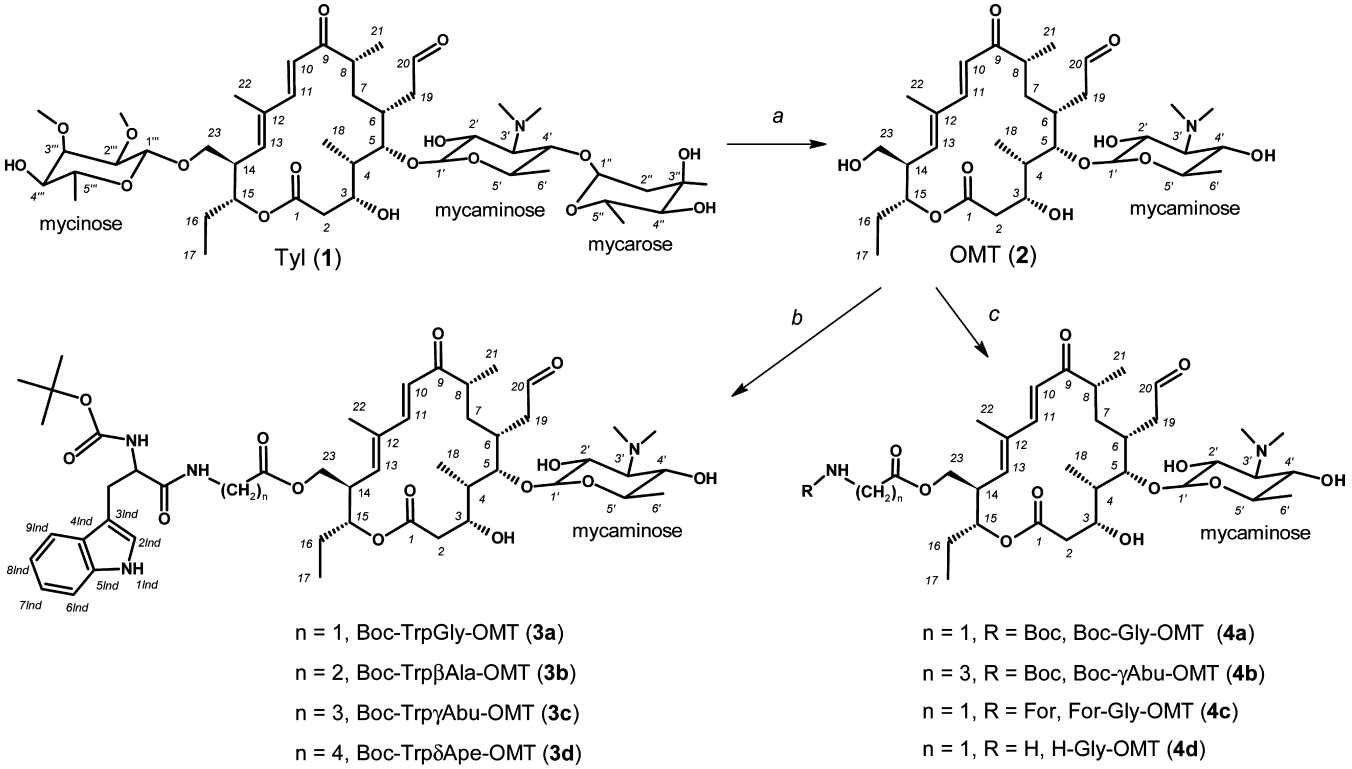

Figure 2. Synthesis of 5-*O*-mycaminosyltylonolide (OMT, **2**) and its derivatives **3a**−**3d** and **4a**−**4d**: (a) H_2SO_4 aq, reflux, 50 h; (b) Boc-TrpGly-OH (Boc-Trp*β*Ala-OH, Boc-Trp*γ*Abu-OH, Boc-Trp*δ*Ape-OH), DCC (1.5 equiv), DMAP (0.5 equiv), CH_2Cl_2, 8−12 h; (c) (1) Boc-Gly-OH (Boc-*γ*Abu-OH, For-Gly-OH), DCC (1 equiv), DMAP (1.5 equiv), CH_2Cl_2 (DMF/CH_2Cl_2), 8−12 h, (2) TFA (**4d**).

crystallographic analysis (reviewed[5,6]). It was understood that the carbohydrate residues of macrolides are extended along the NPET walls, whereas the lactone ring forms numerous contacts with the NPET surface and fills the substantial part of the NPET lumen.[7] Moreover, it was recently discovered that at least some of macrolides are able to inhibit synthesis only if they recognize (directly or allosterically) specific amino acid sequences in the growing polypeptide chain.[8] The understanding of these complex interdependent relations between NPET wall elements, antibiotics, and the nascent chain remains very limited. At the same time elucidation of this problem will facilitate future development of ribosome-targeted drugs.

dx.doi.org/10.1021/bc400236n | *Bioconjugate Chem.* 2013, 24, 1861−1869

With this goal in mind, we have previously designed and prepared a number of tylosin (Figure 1, **1**), desmycosin, and 5-*O*-mycominosyltylonolide (OMT) (Figure 1, **2**) peptide derivatives.[9−12] The peptide portion of these molecules models elements of a growing polypeptide chain, whereas the antibiotic part serves as an ″anchor″ for positioning the peptide at a specific site of NPET. In particular, it was shown that amino acids and peptides attached to the C20 aldehyde position of tylosin could be useful instruments for monitoring the first (next to PTC) regulatory region of NPET.[12]

In this paper we report on the syntheses and properties of novel C23 OMT derivatives containing amino acid and dipeptide moieties. We assume that these compounds could be used as new probes for studying NC sequence specific and nonspecific interactions with the second (more remote from the PTC) regulatory region of NPET located in its narrowest segment. It was established in the case of the best-studied stalling peptides, TnaC and SecM, that the tryptophan residues critical for stalling are located at this NPET region.[13−16] Because of that, tryptophan derivatives placed at different distances from the macrolide lactone were included in the list of compounds for conjugation with OMT.

MATERIALS AND METHODS

Synthesis. The following reagents were used: amino acid derivatives (Fluka); benzotriazol-1-yloxy-tris(dimethylamino)-phosphonium hexafluorophosphate (BOP), DCC and DMAP (Merck), tylosin (Mosagrogen, Russia). TLC was carried out on 0.2 mm precoated plates of silica gel 60 F254 (Merck), column chromatography, on silica gel 60 (0.063−0.2 mm) (Merck). The following solvents systems were used: (1) chloroform:methanol:water, 65:25:4; (2) chloroform:methanol:water:ethyl acetate, 20:6:1:0.3; (3) chloroform:methanol, 4:1; (4) chloroform:methanol, 2:1; (5) dichloromethane:acetone:methanol, 7:3:0.5. Spots were visualized by UV, ninhydrin, and 2,4-dinitrophenylhydrazine reagents.

NMR spectra were recorded on Bruker AV 600 (600 MHz for ^{1}H and 150.91 MHz for ^{13}C; 303 K) and DRX 400 (400 MHz for ^{1}H; 300 K). The chemical shift values are reported as δ ppm relative to TMS used as internal standard and the coupling constants (J) are measured in Hz. Mass spectra were recorded on the LC-MS with the ionization mode APCI (Agilent, USA) equipped with 4.6 × 50 mm column Onix Monolithic C18 (I) and the UPLC/MS/MS system consisted of Acquity UPLC system (Waters, USA) equipped with 2.1 × 50 mm column Acquity BEH C18 1.7 um, diode array detector scanning at 200−500 nm and tandem quadrupole mass spectrometer TQD (Waters, USA) with the ESI-ionization (II). The data for the predominant monoisotope peak and retention time (τ) in a gradient 5−95% of B in A for 2.4 min: (A) 0.1% TFA in water and (B) 0.1% TFA in acetonitrile (elution rate 3.55 mL/min; 25 °C), for LC-MS-system I; and in a gradient 5−100% of B in A for 3 min: (A) 20 mM formic acid in water and (B) 20 mM formic acid in acetonitrile (elution rate 0.5 mL/min; 35 °C), for LC-MS-system II are presented.

General Synthetic Procedures. General scheme for the synthesis of OMT C23-derivatives (**3a−d**, **4a−d**) is represented in Figure 2. See also Supporting Information for more detailed procedures and NMR data.

*23-O-(N-tert-Butyloxycarbonyl-L-tryptophanylglycyl)-OMT (**3a**).* To a solution of 70 mg (0.117 mmol) of **2**, 46.5 mg (0.129 mmol) of Boc-TrpGly-OH in 1 mL of methylene chloride solutions of DMAP (8.6 mg, 0.070 mmol) and DCC (30.0 mg, 0.145 mmol) in 600 and 400 μL of methylene chloride, respectively, were added by portions for 4 h under stirring and cooling (0 °C), and stirring was continued for 5 h at 0 °C. Then the reaction mixture was filtered, methylene chloride was evaporated *in vacuo*, and the residue was chromatographed in system (1), affording **3a** as white powder (60 mg, 54% yield). R_f(1) 0.64. LC-MS: τ 1.607 min (I), m/z = 941.37 $[M+H]^+$ (calc. for $C_{49}H_{72}N_4O_{14}$ 940.50).

*23-O-(N-tert-Butyloxycarbonyl-L-tryptophanyl-β-alanyl)-OMT (**3b**).* This was obtained starting from **2** (10.2 mg, 17 μmol), Boc-TrpβAla-OH (7.5 mg, 20 μmol), DCC (40 μmol), and DMAP (17 μmol), according to the procedure used for **3a**. The crude oily product **3b** (13 mg, 80% yield) was purified by CC on silica gel in eluent (2). Then the individual compound **3b** was precipitated by petroleum ether from methylene chloride (10.5 mg, 62%). R_f(2) 0.57. LC-MS: τ 1.56 min (II), m/z = 955.34 $[M+H]^+$ (calc. for $C_{50}H_{74}N_4O_{14}$ 954.52).

*23-O-(N-tert-Butyloxycarbonyl-L-tryptophanyl-γ-aminobutyryl)-OMT (**3c**).* This was obtained starting from **2** (18 mg, 30 μmol), Boc-TrpδAbu-OH (13.7 mg, 35 μmol), DCC (8 mg, 40 μmol), and DMAP (2 mg, 17 μmol) according to the procedure used for **3a** as a white powdery product (15.1 mg, 52% yield after CC purification in system (2)). R_f(2) 0.65. LC-MS: τ 1.591 min (I), τ 1.66 min (II), m/z = 969.48 $[M+H]^+$ (calc. for $C_{51}H_{76}N_4O_{14}$ 968.54).

*23-O-(N-tert-Butyloxycarbonyl-L-tryptophanyl-δ-aminopentanoyl)-OMT (**3d**).* This was obtained starting from **2** (18 mg, 30 μmol), Boc-TrpγApe−OH (16.2 mg, 40 μmol), DCC (15.3 mg, 74 μmol), and DMAP (3.9 mg 32 μmol); according to the procedure used for **3a**, compound **3d** was obtained as a white powdery substance (15 mg, 45% yield after purification in system (2)). R_f(2) 0.68. LC-MS: τ 1.626 min (I), m/z = 983.34 $[M+H]^+$ (calc. for $C_{52}H_{78}N_4O_{14}$ 982.55).

*23-O-(N-tert-Butyloxycarbonyl-glycyl)-OMT (**4a**).* This was synthesized according to the procedure used for **3a** starting from 39.0 mg (0.065 mmol) of **2**, 12 mg (0.07 mmol) of Boc-Gly-OH, 5.0 mg (0.04 mmol) of DMAP, and 21 mg (0.10 mmol) of DCC. The product was purified using CC in system (2), affording **4a** (26 mg, 53% yield). R_f (2) 0.66. LC-MS: τ 1.52 min (II), m/z = 755.51 $[M+H]^+$ (calc. for $C_{38}H_{62}N_2O_{13}$ 754.34).

*23-O-(N-Formyl-glycyl)-OMT (**4c**).* This was synthesized according to the procedure used for **3a** starting from 57.0 mg (0.09 mmol) of **2**, 13.2 mg (0.13 mmol) of For-Gly-OH, 7.3 mg (0.06) of DMAP, and 31 mg (0.15 mmol) of DCC. The product was purified using CC in system (3), affording **4c** (21 mg, 34% yield). R_f (3) 0.33. LC-MS: τ 1.03 min (II), m/z = 683.78 $[M+H]^+$ (calc. for $C_{34}H_{54}N_2O_{12}$ 682.37).

*23-O-Glycyl-OMT Trifluoroacetate (**4d**).* A solution of 10 mg (13 μmol) of **4a** in a mixture of 130 μL TFA and 550 μL CH_2Cl_2 was kept at 0 °C for 1 h, then 100 μL of TFA was added, and the reaction mixture was kept for 10 min at room temperature and for 10 min at 4 °C, evaporated *in vacuo*, and the residue was purified using CC in system (4) to give 3 mg (30% yield) of **4d**. R_f(4) 0.20. LC-MS: τ 0.84 min (II), m/z = 655.45 $[M+H]^+$ (calc. for $C_{33}H_{54}N_2O_{11}$ 654.74).

Translation Inhibition Assay. Translation in *E. coli* (*strain* A19) S30 extract was carried out as described[17] at 25 °C in the presence of 1.2 mM ATP, 0.8 mM GTP, CTP, and UTP each, 0.03 mg/mL folinic acid, 80 mM creatine phosphate, 0.25 mg/mL creatine kinase, 0.64 mM cAMP, 4% PEG 8000, 1 mM amino acids each except glutamic acid, and 0.175 mg/mL total *E. coli* tRNA in a buffer containing 14.8 mM $Mg(OAc)_2$, 26

dx.doi.org/10.1021/bc400236n | *Bioconjugate Chem.* 2013, 24, 1861−1869

mM HEPES-KOH (pH_{20} 7.5), 27.5 mM KOAc, 210 mM potassium glutamate, and 1.7 mM dithiothreitol. The reaction mixture also contained 0.1 mM luciferin. Antibiotics were added in the following final concentrations: 1.0, 3.0, and 9.0 μM. The reaction mixture was preincubated at 25 °C for 2 min, and then translation was initiated by addition of luciferase mRNA to the concentration of 20 mg/mL.

Binding Assay. *Fluorescence Polarization.* 70S ribosomes were prepared from an *E. coli* strain BW25113.[18] Fluorescence polarization (FP) displacement assay was done according to the procedure described.[19] *E. coli* ribosomes were incubated at 37 °C for 15 min and then diluted in a binding buffer (20 mM HEPES, pH 7.5, 50 mM NH_4Cl, 10 mM $MgCl_2$, 4 mM β-ME, 0.05% (v/v) Tween 20). BODIPY-erythromycin (10 nM), prepared as described,[19] was preincubated with the ribosomes (7 nM) for 30 min. The optimal concentration of the ribosomes was calculated on the basis of mathematical simulations (Advanced Grapher 2.2).[20] Then a compound, diluted in binding buffer, in a series of concentrations was mixed with 24 μL of the above-described ligand−ribosome mixture to the total volume 50 μL in a 384-well plate and incubated at room temperature for 2 h. FP values (mP) were measured using an Perkin-Elmer VICTOR X5 Multilabel Plate Reader (excitation at 485 nm and emission at 535 nm). *G* factor correction was performed using a fluorescein standard. Data acquisition times were 0.1 s/well using a *z* working height of 8 mm.

Data Analysis. The binding data were fit to a cubic equation (GraphPad Prizm 6) that solves the dissociation constant of the unlabeled compound−ribosome complex (K_D^{RB}) for a single binding site with two competitive ligands[21] (see also Supporting Information for more detailed binding data analysis). The dissociation constant of the BODIPY-erythromycin-ribosome complex (K_D^{RA}) was assumed to be 20 nM.[19] In the FP displacement assay, the K_Ds were obtained from 6 replicates. The K_Ds given in the text are the means ±95% confidence intervals.

Molecular Dynamics Simulation. *Simulated System.* The structure of *E. coli* ribosome was derived from the 3.1 Å resolution X-ray structure (PDB code: 3OFR)[22] with addition of modified bases to 23S rRNA in compliance with database.[23] Modified base positions were optimized by combination of steepest descent/l-bfgs energy minimization[24] with further short molecular dynamics simulation. During these procedures all nonmodified residues were fixed, whereas modified bases, water, and ions were free. The structure of the complex of tylosin with the large ribosomal subunit was obtained by superposition and universally conserved bases A2100, A2101, G2102, A2103, and A2538 derived from the 3.0 Å resolution X-ray structure of *H. marismortui* (PDB code: 1K9M)[7] on respective A2059, A2060, G2061, A2062, and A2503 bases derived from the structure of *E. coli* ribosome mentioned above. This structure was superimposed on the structure of the large ribosomal subunit of the *E. coli* ribosome with included modified bases to obtain structure of macrolide complex containing modifications in 23S rRNA. Then all residues that had at least one atom within a cubic area with 7 nm edge including whole ribosome tunnel and bound tylosin were selected, in which the connection center of this cubic area was situated at the tunnel and the tunnel went along the imaginary *Z*-axis of this area. This selection was used for molecular dynamic simulation. Systems containing OMT and its derivatives (Boc-Gly-OMT, Boc-γAbu-OMT) were made by superimposition these derivatives structures on the tylosin structure.

Simulation Details. All molecular dynamics simulations and analysis of MD trajectories were carried out using the GROMACS[25,26] 4.5.4 software package and parm99sb force field. All simulations were performed at T = 300 K with a time constant for coupling of 0.1 ps under the control of a velocity rescaling thermostat with additional stochastic term,[27] and isotropic constant-pressure boundary conditions under the control of the Berendsen algorithm of pressure coupling[28] with a time constant of 5 ps and application of the particle mesh Ewald method for electrostatic interactions (PME)[29] with grid spacing of 0.125 nm and interpolation order 4. A cubic box with 8.8 nm edge containing centered simulated system was filled by TIP4P[30] water molecules, so faces of the system were covered by 0.9 nm of solvent. Negative charges were neutralized with the addition of magnesium and sodium counterions, since application of potassium ions as counterions will lead to greater perturbations in modeled structure than sodium ions do.[31] Magnesium cations were added so as to form "magnesium bridges" between adjacent phosphate groups and residual negative charges were compensated by sodium cations located nearby negatively charged group[32] (script was generously provided by A. Zalevsky). Residues that had at least one atom within 0.1 nm from the face of a selected fragment of ribosome were positionally restrained, but all the rest were left nonrestrained. The time step for integration in all simulation was 2 fs; coordinates were written to output a trajectory file (saved system configuration or frame) every 60 ps. Trajectories calculated were 500 ns long for all compounds. An H-bond was treated as existing if hydrogen donor and acceptor atoms were closer than 0.35 nm and the angle between the line connecting these atoms and the bond to the hydrogen atom covalently linked to the donor atom was lower than 30°.

RESULTS

The antibiotic OMT is a precursor in the biosynthesis of the classical 16-membered macrolide tylosin. Unlike tylosin, OMT contains a single carbohydrate residue, mycaminose, at position C5 of the lacton ring and a reactive hydroxy group at position C23 (Figure 1, **2**). The absence of the mycinose residue in OMT opens up an excellent way to put amino acid or peptide residues at its vacant place.

Synthesis. OMT was obtained by acidic hydrolysis of tylosin as described earlier.[33] Our strategy of the preparation of OMT peptide derivatives was partially developed in the previous study.[10] In the case of OMT derivatives bearing Trp this approach allowed a relatively simple synthesis (Figure 2). The final step was the introduction of *N*-protected Trp derivatives to the macrolide molecule. The tryptophan derivatives used in this study contained Boc-Trp as an *N*-terminal residue and an optically inactive amino acid of the general formula $H_2N(CH_2)_nCOOH$ with n equal to 1 (glycine), 2 (β-alanine), 3 (γ-aminobutyric acid), or 4 (δ-aminopentanoic acid) as a linker of variable length. The primary C23 hydroxyl group of OMT can be selectively acylated without preliminary protection of the mycaminose hydroxyl groups. Previously, OMT was reported to be preferentially acylated at the C23 hydroxyl by acid chloroanhydrides.[34] Our method is less laborious since it permits the use of modifiers with a free carboxylic function in order to acylate the C23 hydroxyl group. Using optically inactive amino acid residues at the C-terminus of the dipeptide allowed us to overcome difficulties caused by

racemization during the condensation reaction. Another advantage of our synthetic strategy is the possibility of using unprotected OMT. The structures of OMT and all its derivatives were confirmed by ESI-MS mass spectrometry and ^{1}H and ^{13}C NMR spectra.

In Vitro Inhibitory Activity and Binding. The peptide derivatives of OMT were tested for their ability to inhibit translation of firefly luciferase mRNA *in vitro* in *E. coli* S30 extract, in which the synthesis of luciferase was monitored by luminescence.[17]

As follows from Figure 3 all the Trp-containing OMT derivatives proven to be potent inhibitors of the luciferase synthesis. However, most OMT derivatives exhibited a lower (although comparable) inhibitory activity than unmodified antibiotic. An important exception was Boc-TrpGly-OMT, which was more potent than the initial antibiotic. To evaluate the impact of the hydrophobic *tert*-butyloxycarbonyl protection group and the residue that links Trp to the C23 position of OMT on the inhibitory activity of OMT-derivatives, we prepared Boc-Gly- and For-Gly-OMT derivatives (Figure 2, **4a** and **4c**) as well as Boc-γ-aminobutyryl-OMT and unprotected Gly-OMT (Figure 2, **4b** and **4d**). The unprotected Gly-OMT was a poor inhibitor of luciferase synthesis (the residual luciferase activity was about 90% at the inhibitor concentration of 3 μM) possibly due to electrostatic repulsion between the free amino group of Gly and the ε-amino group of Lys90 of ribosomal protein L22, which could be located in close proximity to each other. Both Boc-Gly-OMT and For-Gly-OMT proved to be unexpectedly potent inhibitors, somewhat more potent than unmodified OMT (Figure 3). The inhibitory activity of Boc-γ-aminobutyryl-OMT was much lower.

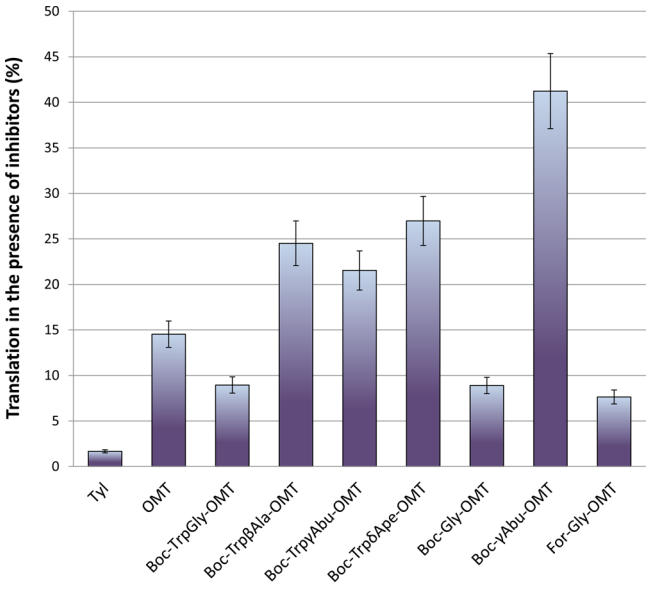

Figure 3. Inhibition of the firefly luciferase mRNA translation in *E. coli* S30 extracts in the presence of tylosin, OMT, and OMT derivatives at a concentration of 3 μM. The bars represent the mean value of the relative residual activity of luciferase in three independent experiments.

Boc-Gly-OMT and OMT were found to efficiently compete with the fluorescently labeled erythromycin in ribosome binding. The data of Boc-Gly-OMT binding to *E. coli* 70S ribosome analyzed using the FP-based competition with BODIPY-erythromycin[19] demonstrated that Boc-Gly-OMT interacts with the ribosomes much stronger than OMT: the values of the dissociation constants (K_Ds) of the macrolide–ribosome complexes are 0.19 ± 0.27 nM and 1.86 ± 0.67 nM for Boc-Gly-OMT and OMT, respectively. It is worth mentioning that the use of BODIPY-derivative of tylosin instead of BODIPY-erythromycin in FP-based competition experiments revealed approximately the same difference in K_D values of Boc-Gly-OMT and OMT complexes with the *E. coli* ribosomes (unpublished results).

In an attempt to rationalize these results we performed MD simulation of ribosomal tunnel complexes with tylosin, unmodified OMT, and its conjugates with Boc-glycine and

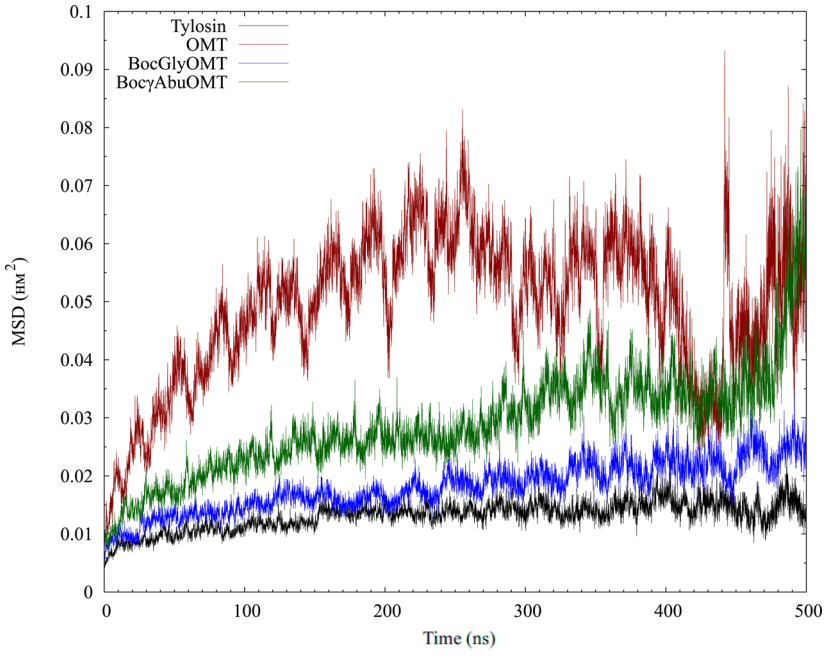

Figure 4. Mean-squared deviation plots for tylosine, OMT, and its derivatives in the *E. coli* ribosomal tunnel over simulation time.

dx.doi.org/10.1021/bc400236n | *Bioconjugate Chem.* 2013, 24, 1861–1869

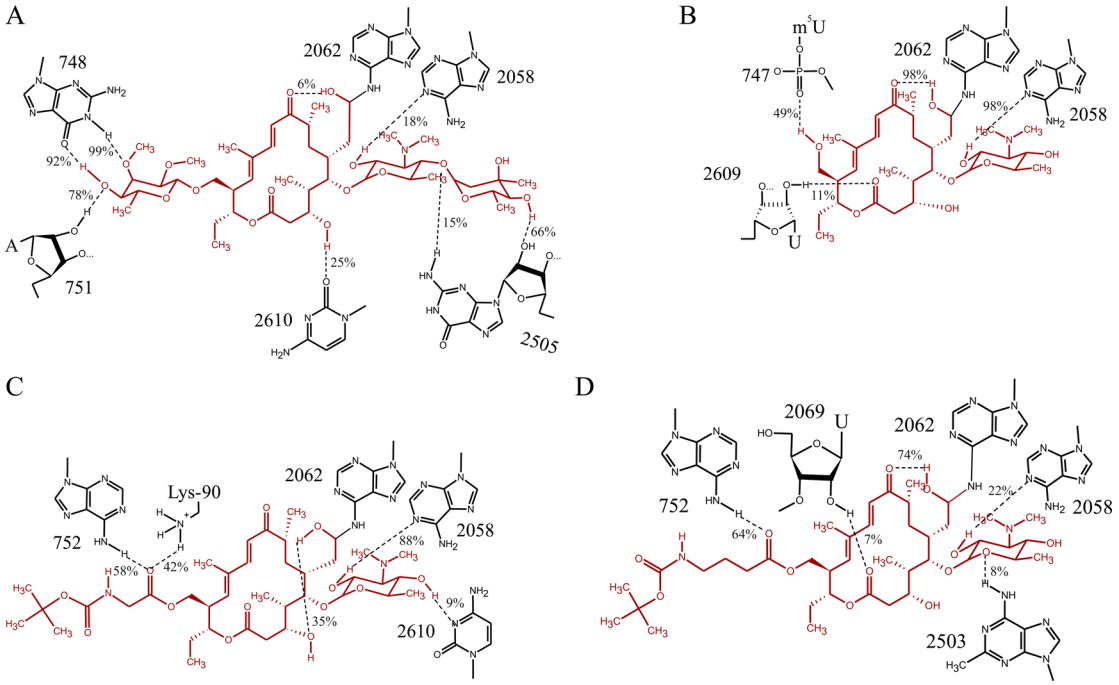

Figure 5. Chemical structure diagram of tylosine (A), OMT (B), Boc-Gly-OMT (C), and Boc-γAbu-OMT (D) showing hydrogen-bonding of their reactive groups with 23S rRNA nucleotides and Lys90 of protein L22 in the exit tunnel of *E. coli* ribosomes. Percent of occurrence of given hydrogen bond is a part of frame in which this hydrogen bond is present. Therefore, percent of occurrence is a measure of hydrogen bond stability.

Boc-γ-aminobutyric acid. Above all, we hoped that the MD simulation approach, the increasingly important role of which in ribosome structural studies is evident,[15,16] will help us to understand unexpected behavior of *N*-acyl-Gly-containing derivatives of OMT.

Molecular Dynamics Simulation. Previously, MD was successfully used for characterization of NPET interaction with a variety of ligands including some macrolides[35] and nascent polypeptide chains.[15,16,36] However, to the best of our knowledge, it has never been applied to ribosome complexes with macrolides of the tylosin family. The key idea of our approach was to extract the cubic neighborhood around a macrolide or its derivative and apply position restraints on the edge atoms of the cubic part of ribosome around the macrolide, while the ribosome atoms located in close proximity to the ligand and ligand itself were allowed to move freely. The major difference from a previously published similar approach[36] is the use of cubic extraction, minimization of additional volume occupied by water molecules, and keeping ribosome highly charged surrounding through periodic boundary conditions.

To make sure that this approach was relevant to our goal, we first applied these conditions to the complex of tylosin with 50S subunit from *Haloarcula marismortui* (PDB ID 1K9M).[7] The selected parameter for the examination of the stability of the tylosin complex with the ribosome was the mean square displacement of macrolide ring (MSD) between current and starting structures, following least-squares fitting. Large MSD values for the tylosin ring would indicate that the complex structure is heavily disrupted during MD simulation. In our simulation tylosin covalently bonded to the ribosome demonstrated very moderate movement of the lactone ring in an observed time of 450 ns (0.015 nm^2). This observation supports the suitability of our approach for treating ribosome environment in used sampling time with reasonable computational resources. Actually, as illustrated in Figure 4, MSD values for tylosin and OMT and its derivatives, superimposed onto erythromycin in the 50S subunit of the *E. coli* ribosome, were not too high: MSD values for tylosin and Boc-Gly-OMT were only 0.01 nm^2, about 0.03 nm^2 for Boc-γ-aminobutyryl-OMT and 0.06 nm^2 for unmodified OMT.

The displacement of the macrolide ring of tylosin is lower than that of OMT due to interactions of two additional sugar residues of tylosin with NPET walls. In particular, as could be seen in Figure 5A, the mycinose residue of tylosin forms three very stable hydrogen bonds with G748 and A751 of 23S rRNA of the *E. coli* ribosomes. In contrast OMT forms only one very stable hydrogen bond with a NPET residue (Figure 5B) that can be the reason for its relatively high flexibility (Figure 4).

It is remarkable that MSD values for Boc-Gly-OMT are comparable with those for tylosin in the *E. coli* ribosome and are considerably lower than those for unmodified OMT. This finding may also indicate the formation of an efficient hydrogen bonding network by Boc-Gly group. Hence, we found that the carbonyl group of the glycine residue in Boc-Gly-OMT forms two hydrogen bonds – with the ε-amino group of Lys 90 of protein L22 and A752 of the 23S rRNA (Figure 5C). This observation is consistent with well-known ability of carbonyl oxygens to simultaneously form two H-bonds due to sterical availability. The percentage occupancy of these hydrogen bonds was 42 and 58, respectively. In contrast to Boc-Gly-OMT, in Boc-γ-aminobutyryl-OMT the carbonyl group of γ-aminobutyric acid residue may form only one stable H-bond with A752 (Figure 5D); it does not form a hydrogen bond with Lys90 due to a freely moving Boc-γ-aminobutyryl group that can reach the hydrophobic surface of G748 by maximal displacement of antibiotic stacking to this hydrophobic surface, thereby resulting in nonspecific hydrophobic contact. At the same time, the Boc protective group in Boc-Gly-OMT appeared to be uninvolved in any strong hydrophobic interactions. This explains why the mean square displacement

dx.doi.org/10.1021/bc400236n | *Bioconjugate Chem.* 2013, 24, 1861–1869

of Boc-γ-AbuOMT lactone ring is larger than that of Boc-Gly-OMT (Figure 4).

All compounds form an intramolecular hydrogen bond between the OH-group of the carbinolamino bridge connecting a macrolide with A2062 and either O3 or O9 atoms of macrolactone ring (Figure 5). It is not clear however what role this bond plays in stabilization of macrolide−ribosome complexes.

DISCUSSION

The preparation method for the C23 derivatives of OMT, which was developed in our previous research[10] and refined in this study, allowed us to synthesize in satisfactory yields a series of compounds with Trp residues located at different distances from the tylonolide ring. Although no crystal structure of a complex of OMT with the ribosome is available it was conclusively demonstrated that the lactone rings of tylosin and OMT are similarly positioned in NPET.[37] Analysis of the X-ray structure of tylosin bound to the 50S subunit of the ribosome from *Haloarcula marismortui*[7] and a cryo-electron microscopy structure of TnaC in NPET of *E. coli* ribosomes[15] as well as an array of biochemical and genetic data (recently reviewed[38]) suggested that the binding site of the tylosin mycinose residue in the antibiotic−ribosome complex overlaps with the binding region of the tryptophan residue in the NPET that is critical for TnaC-mediated stalling. This site is composed of the A748-A752 region of 23S rRNA and the amino acid residues of the ribosomal protein L22, located at the beta-hairpin tip of its extended loop. Some of these nucleotide and amino acid residues were proven to be crucial for functionally important interactions of TnaC with NPET.[13]

It was expected that Trp-OMT derivatives prepared in this study would demonstrate substantial ability to inhibit protein synthesis *in vitro*. Data presented in Figure 3 indicate that indeed Boc-TrpGly-OMT has a higher potency than unmodified OMT. We initially supposed that this effect was due to interaction of the Trp aromatic residue in Boc-TrpGly-OMT with a still unknown "Trp-recognition" site at NPET walls. However, further experiments with Gly derivatives of OMT lacking the Trp residue (Figure 3) clearly demonstrated that it was the *N*-acylated glycine fragment of Boc-TrpGly-OMT that was responsible for its high inhibitory activity. Moreover, we have found that the bulky hydrophobic *N*-protection group in Boc-Gly-OMT could be replaced with a hydrophilic formyl group without alteration of its ability to suppress luciferase synthesis.

Thus, all three *N*-acyl-Gly-containing derivatives of OMT used in this study demonstrated much higher inhibitory activity in cell free system than their parental macrolide (OMT) (Figure 3).

The tylosin-related class of macrolides as well as other C6 acetaldehyde-containing macrolides with a 16-membered lactone ring represent a special family of ribosomal antibiotics. In the course of binding to the ribosome they form a reversible covalent bond with N6 of A2062 of 23S rRNA by means of their aldehyde group.[7] It has been known for a long time that conversion of the C20 aldehyde group of tylosin, desmycosin, OMT, and their analogs into the corresponding C20 hydroxyl or methyl groups led to a substantial loss of their antimicrobial activity (ref 39 and references therein). We have recently shown that reduction of the aldehyde group of tylosin dramatically decreased its ability to compete with erythromycin for ribosome binding and turned this antibiotic into a very poor inhibitor of the *in vitro* synthesis of green fluorescent protein,[12] reaffirming its importance. However, the efficient formation of a covalent bond between the C20 aldehyde group of an antibiotic and the amino group of A2062 requires an appropriate mutual orientation of these partners that is probably achieved owing to a network of hydrogen bonds formed by the macrolide with the NPET walls. Therefore, comparing the results obtained in the course of MD simulations of ribosome complexes with strong (tylosin, Boc-Gly-OMT) and relatively weak (OMT, Boc-γ-aminobutyryl-OMT) inhibitors of luciferase synthesis, we focused on the identification of the hydrogen bonds which these OMT-derivatives form with elements of NPET walls and on the estimation of H-bond lifetimes.

It is worth noting that binding of macrolide antibiotics with NPET is at least a two-step process with complicated kinetics.[40] At the same time, the simulation system used in this work represents the so-called ground-state complex of an inhibitor with the ribosome derived from the crystalline structure of the tylosin complex with *Haloarcula marismortiu* ribosomes.[7] Therefore, it was not evident *a priori* that analysis of MD simulation data would directly correlate with experimental results obtained in this study. However, comparison of inhibitory activity of tylosin, OMT, and its derivatives (Figure 3) with arrangement and percentage occupancy of hydrogen bonds formed between these compounds and NPET walls during MD simulations (Figure 5) enabled a plausible explanation for variations in their ability to inhibit translation and, in particular, to explain high inhibitory activities of *N*-acylglycyl-containing compounds. The *N*-acylglycyl moiety, which closely resembles the backbone of a polypeptide chain, forms two stable hydrogen bonds with the nucleotide residue of A752 of 23S rRNA and the Lys 90 residue of the ribosomal protein L22 (Figure 5C). It is known that the A752 nucleotide produces a base pair with U2609. The pair is an essential structural and functional element of the ribosomal exit tunnel.[22] It is involved in interactions with both stalling peptides[38] and macrolide antibiotics.[37,41−43] From a different aspect, the functional importance of Lys90 of the protein L22 is also well-established: its mutations eliminate numerous effects associated with TnaC stalling activity.[44]

Thus, in this study we demonstrated once again that amino acid and peptide conjugates with macrolide antibiotics are useful tools for searching of feasible sites of interaction of a growing polypeptide chain with the ribosomal exit tunnel. In particular, biochemical and computational data gathered in this study with the help of Gly-containing derivatives of OMT allow us to propose that the A752 − Lys90 (L22) −element of NPET forms a novel site of interactions with the backbone of a growing polypeptide chain. Earlier, we described the contact which every amino acid residue of NC should form with the nucleotide G2061 of 23S rRNA located in the close proximity to PTC.[45] It is obvious that the strength of these interactions should vary depending on the nature amino acid side chain (e.g., its charge or hydrophobicity). These contacts could modulate a nascent chain conformation (for instance, to keep C-terminal part of NC in an extended form as it was demonstrated for TnaC and *E. coli* ribosome NPET[15]) and the rhythm of passage of a growing polypeptide through NPET. Consequently, they could affect the process of protein maturation and folding at the ribosome tunnel exit. Lastly, in this work we have found for the first time that conjugation of a

macrolide with a single amino acid residue might appreciably increase its potency to inhibit protein synthesis.

■ ASSOCIATED CONTENT

Supporting Information

Details on the synthesis of OMT and tryptophan containing peptides; NMR data for derivatives of OMT; binding assay data analysis. This material is available free of charge via the Internet at http://pubs.acs.org.

■ AUTHOR INFORMATION

Corresponding Author

*Tel.: 7 495 9393143; fax: 7 495 9393181. E-mail address: bogdanov@belozersky.msu.ru.

Author Contributions

Anna Shishkina and Gennady Makarov made an equal contribution to this work.

Notes

The authors declare no competing financial interest.

■ ACKNOWLEDGMENTS

The authors acknowledge the use of "Lomonosov" supercomputer facilities provided by the Moscow State University Computing Center. We thank Vadim Tashlitsky for LC-MS analyses. We thank Vjacheslav Kolb for his help with the antibiotic inhibitory assay and useful discussions. We would like to thank Prof. Alexander Mankin for critical reading of this paper and editing of manuscript. We thank Dr. Bo Liu for his thoughtful discussion of our MD data and useful advice. This work was supported by grants from the Russian Foundation for Basic Researches (10-04-01187, 12-04-31558, and 13-04-00986).

■ ABBREVIATIONS:

CC, column chromatography; DCC, 1,3-dicyclohexylcarbodiimide; DMAP, *N,N*-dimethylaminopyridine; FP, fluorescence polarization; MD, molecular dynamics; MSD, mean square displacement; NC, nascent polypeptide chain; NPET, nascent peptide exit tunnel; OMT, 5-*O*-mycaminosyltylonolide; PTC, peptidyl transferase center; TFA, trifluoroacetic acid

■ REFERENCES

(1) Mankin, A. S. (2006) Nascent peptide in the "birth canal" of the ribosome. *Trends Biochem. Sci. 31*, 11−13.

(2) Bogdanov, A. A., Sumbatyan, N. V., Shishkina, A. V., Karpenko, V. V., and Korshunova, G. A. (2010) Ribosomal tunnel and translation regulation. *Biochemistry (Moscow) 75*, 1501−1516.

(3) Cruz-Vera, L. R., Sachs, M. S., Sguires, C. L., and Yanofsky, C. (2011) Nascent polypeptide sequences that influence ribosome function. *Curr. Opin. Microbiol. 14*, 160−166.

(4) Omura, S. (2002) *Macrolide Antibiotics: Chemistry, Biology and Practice*, Academic Press, Orlando.

(5) Wilson, D. N. (2011) On the specificity of antibiotics targeting the large ribosomal subunit. *Ann. N.Y. Acad. Sci. 1241*, 1−16.

(6) Kannan, K., and Mankin, A. S. (2011) Macrolide antibiotics in the ribosomal tunnel: species-specific binding and action. *Ann. N.Y. Acad. Sci. 1241*, 33−47.

(7) Hansen, J. L., Ippolito, J. A., Ban, N., Nissen, P., Moore, P. B., and Steitz, T. A. (2002) The structures of four macrolide antibiotics bound to the large ribosomal subunit. *Mol. Cell 10*, 117−128.

(8) Kannan, K., Vasquez, N., and Mankin, A. S. (2012) Selective protein synthesis by ribosomes with drug-obstructed exit tunnel. *Cell 151*, 508−520.

(9) Sumbatyan, N. V., Korshunova, G. A., and Bogdanov, A. A. (2003) Peptide derivatives of antibiotics tylosin and desmycosin, protein synthesis inhibitors. *Biochemistry (Moscow) 68*, 1156−1158.

(10) Korshunova, G. A., Sumbatyan, N. V., Fedorova, N. V., Kuznetsova, I. V., Shishkina, A. V., and Bogdanov, A. A. (2007) Peptide derivatives of tylosin-related macrolides. *Russian J. Bioorg. Chem. 33*, 218−226.

(11) Sumbatyan, N. V., Kuznetsova, I. V., Karpenko, V. V., Fedorova, N. V., Chertkov, V. A., Korshunova, G. A., and Bogdanov, A. A. (2010) Amino acid and peptide derivatives of the tylosin family of antibiotics modified by aldehyde function. *Russian J. Bioorg. Chem. 36*, 245−256.

(12) Starosta, A. L., Karpenko, V. V., Shishkina, A. V., Mikolajka, A., Sumbatyan, N. V., Schluenzen, F., Korshunova, G. A., Bogdanov, A. A., and Wilson, D. N. (2010) Interplay between the ribosomal tunnel, nascent chain, and macrolides influences drug inhibition. *Chem. Biol. 17*, 504−514.

(13) Yanofsky, C. (2007) RNA-based regulation of genes of tryptophan synthesis and degradation, in bacteria. *RNA 13*, 1141−1154.

(14) Nakatogawa, H., and Ito, K. (2002) The ribosomal exit tunnel functions as a discriminating gate. *Cell 108*, 629−636.

(15) Seidelt, B., Innis, C. A., Wilson, D. N., Gartmann, M., Armache, J.-P., Villa, L., Trabuco, L. G., Becker, T., Mielke, T., Schulten, K., Steitz, T. A., and Beckmann, R. (2009) Structural insight into nascent polypeptide chain−mediated translational stalling. *Science 326*, 1412−1415.

(16) Gumbert, J., Schreiner, G. J., Wilson, D. N., Beckmann, R., and Schulten, K. (2012) Mechanism of SecM-mediated stalling in the ribosome. *Biophys. J. 103*, 331−341.

(17) Svetlov, M. S., Kommer, A., Kolb, V. A., and Spirin, A. S. (2006) Effective cotranslational folding of firefly luciferase without chaperones of the Hsp70 family. *Protein Sci. 15*, 242−247.

(18) Noll, M., Hapke, B., and Noll, H. (1973) Structural dynamics of bacterial ribosomes, II. Preparation and characterization of ribosomes and subunits in the translation of natural messenger RNA. *J. Mol. Biol. 80*, 519−529.

(19) Yan, K., Hunt, E., Berge, J., May, E., Copeland, R. A., and Gontarek, R. R. (2005) Fluorescence polarization method to characterize macrolide-ribosome interactions. *Antimicrob. Agents Chemother. 49*, 3367−3372.

(20) Roehrl, M. H., Wang, J. Y., and Wagner, G. (2004) A general framework for development and data analysis of competitive high-throughput screens for small-molecule inhibitors of protein-protein interactions by fluorescence polarization. *Biochemistry 43*, 16056−16066.

(21) Wang, Z. X. (1995) An exact mathematical expression for describing competitive binding of two different ligands to a protein molecule. *FEBS Lett. 360*, 111−114.

(22) Dunkle, J. A., Xiong, L., Mankin, A. S., and Cate, J. H. (2010) Structures of the Escherichia coli ribosome with antibiotics bound near the peptidyl transferase center explain spectra of drug action. *Proc. Natl. Acad. Sci. U.S.A. 107*, 17152−17157.

(23) http://www.rna.icmb.utexas.edu/SAE/2A/nt_Modifications/23S-mods

(24) Byrd, R. H., Lu, P., and Nocedal, J. (1995) A limited memory algorithm for bound constrained optimization. *SIAM J. Scientif. Statistic. Comput. 16*, 1190−1208.

(25) Van der Spoel, D., Lindahl, E., Hess, B., Groenhof, G., Mark, A. E., and Berendsen, H. J. C. (2005) GROMACS: Fast, flexible, free. *J. Comput. Chem. 26*, 1701−1718.

(26) Hess, B., Kutzner, C., van der Spoel, D., and Lindahl, E. (2008) GROMACS 4: algorithms for highly efficient, load-balanced, and scalable molecular simulation. *J. Chem. Theory Comput. 4*, 435−447.

(27) Bussi, G., Donadio, D., and Parrinello, M. (2007) Canonical sampling through velocity rescaling. *J. Chem. Phys. 126*, 014107−1−014107−6.

(28) Berendsen, H. J. C., Postma, J. P. M., van Gunsteren, W. F., DiNola, A., and Haak, J. R. (1984) Molecular dynamics with coupling to an external bath. *J. Chem. Phys. 81*, 3684−3690.

(29) Darden, T., York, D., and Pedersen, L. (1993) Particle mesh Ewald: An N log(N) method for Ewald sums in large systems. *J. Chem. Phys. 98*, 10089−10092.
(30) Jorgensen, W. L., Chandrasekhar, J., and Madura, J. D. (1983) Comparison of simple potential functions for simulating liquid water. *J. Chem. Phys. 79*, 926−935.
(31) Reshetnikov, R. V., Sponer, J., Rassokhina, O. I., Kopylov, A. M., Tsvetkov, P. O., Makarov, A. A., and Golovin, A. V. (2011) Cation binding to 15-TBA quadruplex DNA is a multiple-pathway cation-dependent process. *Nucleic Acids Res. 39*, 9789−9802.
(32) Athavale, S. S., Petrov, A. S., Hsiao, C., Watkins, D., Prickett, C. D., Gossett, J. J., Lie, L., Bowman, J. C., O'Neill, E., Bernier, C. R., Hud, N. V., Wartell, R. M., Harvey, S. C., and Williams, L. D. (2012) RNA folding and catalysis mediated by Iron (II). *Plos One 7*, 1−7.
(33) Morin, R., and Gorman, M. (1969) O-Mycaminosyltylonolide and process for the preparation thereof. U.S. Patent 3,459,853.
(34) Kirst, H. A. (1983) OMT ester derivatives. G.B. Patent 2,111,497.
(35) Yam, W. K., and Wahab, H. A. (2009) Molecular insights into 14-membered macrolides using MM-PBSA method. *J. Chem. Inf. Modeling 49*, 1558−1567.
(36) Petrone, P. M., Snow, C. D., Lucent, D., and and Pande, V. S. (2008) Side-chain recognition and gating in the ribosome exit tunnel. *Proc. Natl. Acad. Sci. U.S.A. 105*, 16549−16554.
(37) Karahalios, P., Kalpaxis, D. L., Fu, H., Katz, L., Wilson, D. N., and Dinos, G. P. (2006) On the mechanism of action of 9-O-arylalkyloxime derivatives of 6-O-mycaminosyltylonolide, a new class of 16-membered macrolide antibiotics. *Mol. Pharmacol. 70*, 1271−1280.
(38) Trabuco, L. G., Harrison, B. C., Schreiner, E., and Schulten, K. (2010) Recognition of the regulatory nascent chain tnaC by the ribosome. *Structure 18*, 627−637.
(39) Kirst, H. A., Toth, J. E., Debono, M., Willard, K. E., Truedell, B. A., Ott, J. L., Counter, F. T., Felty-Duckworth, A. M., and Pekarek, R. S. (1988) Synthesis and evaluation of tylosin-related macrolides modified at the aldehyde function: a new series of orally effective antibiotics. *J. Med. Chem. 31*, 1631−1641.
(40) Petropoulos, A. D., Kouvela, E. C., Dinos, G. P., and Kalpaxis, D. (2008) Stepwise binding of tylosin and erythromycin to *Escherichia coli* ribosomes, characterized by kinetic and footprinting analysis. *J. Biol. Chem. 283*, 4756−4765.
(41) Bulkley, D., Innis, C. A., Blaha, G., and Steitz, T. A. (2010) Revisiting the structures of several antibiotics bound to the bacterial ribosome. *Proc. Natl. Acad. Sci. U.S.A. 107*, 17158−17163.
(42) Llano-Sotelo, B., Dunkle, J., Klepacki, D., Zhang, W., Fernandes, P., Cate, J. H. D., and Mankin, A. S. (2010) Binding and action of CEM-101, a new fluoroketolide antibiotic that inhibits protein synthesis. *Antimicrob. Agents Chemother. 54*, 4961−4970.
(43) Poehlsgaard, J., Andersen, N. M., Warrass, R., and Douthwaite, S. (2012) Visualizing the 16-membered ring macrolides tildipirosin and tilmicosin bound to their ribosomal site. *ACS Chem. Biol. 7*, 1351−1355.
(44) Cruz-Vera, L. R., Rajagopal, S., Squires, S., and Yanofsky, C. (2005) Features of the ribosome-peptidyl-tRNA interactions essential for tryptophan induction of tna operon expression. *Mol. Cell 19*, 333−343.
(45) Bogdanov, A. A. (2003) Some structural aspects of the peptidyltransferase reaction. *Mol. Biol. (Moscow) 37*, 511−514.